Acta Cryst. (1967). **23**, 708

Micromorphology of (111) Faces in Diamond Twins

BY FEDERICO BEDARIDA

Istituto di Mineralogia, Università di Genova, Italy

(*Received* 24 *February* 1967)

Some particular features on (111) faces of twinned diamonds are studied. Their influence on the evolution of the shapes of the trigons, which are sometimes not equilateral, is taken into account, and suggestions are put forward regarding the growth mechanism.

Introduction

The study of winged trigons, reported in a previous paper (Bedarida & Komatsu, 1966) has as its object the exploration of the mechanism of the growth of diamond with reference to the presence of very thin layers.

The present study is more general, concerning the layer growth of diamonds. It concerns three samples, twinned on the (111) face, with weights of 0·58, 0·75, 0·85 carat respectively. They are from South African mines and exhibit strong birefringence, evidence of considerable strain in the crystals; surface features only are studied.

Observations

Normal microscopy, phase-contrast microscopy and interferometry have been employed. Fig. 1 shows the wing of a trigon at a magnification of 1000. The layers, which are some tens of Å thick, are clearly seen, as is the sharp edge in the $[\bar{1}2\bar{1}]$ direction. This is the edge frequently formed on the (111) face and it is a ridge. It certainly plays an important part in the dynamics of the phenomenon studied. It is the edge between two stepped vicinal faces and its slope is directly connected with the slope of the two adjacent faces. From a theoretical point of view, the slope may have any value, and in the case of the simplest indices for the adjoining faces, the edge could be that of any elementary form of the cubic system.

The samples examined often show vicinal faces with a very small slope on the (111) face.

It has been possible to measure interferometrically the average slope on the (111) face of the inner walls of many trigons. This is approximately 10°, from which it follows that one can give to those walls an index (332), which is an approximate value since the walls are not perfectly planar.

The geometry of the combination of the wings with the trigon is most frequently that shown in the previous paper, but often not only is the winged trigon symmetrical about a mirror plane $(1\bar{1}0)$, but the trigon itself reduces its threefold symmetry to a mirror symmetry of the same plane such that its profile becomes an isosceles triangle, an example being Fig. 2 in which one side is longer than the other two. Schematically it might be considered that the layers are such as they would be if two of the trigon sides were to rotate, as shown in Fig. 3. This point will be taken up later.

The above situation occurs when the layers are very thin, that is when they are up to some tens of Å thick. For thicker layers (some hundreds of Å or more) no influence on the threefold symmetry of the trigon has been noticed.

Another infrequent type of geometry in the combination of the wings with the trigon has been detected on the (111) face. This appears only near the side of the face (see Fig. 4, upper-left portion). The proposed mechanism is that of Fig. 5. Here too the trigon has lost its threefold symmetry and is again an isosceles triangle, but it differs from that of Fig. 3, for here it appears as if the sides rotate to produce an isosceles triangle with the base smaller than the sides. (The two 'equal' sides also change their lengths but not to the same extent as the base.) The wings of the trigon join

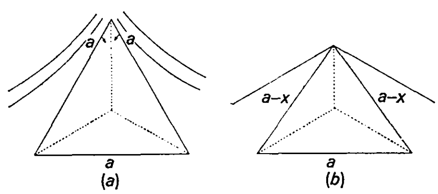

Fig. 3 Diagrams showing schematically the conversion of an equilateral trigon (*a*) into an isosceles trigon (*b*) with the base longer than the other sides.

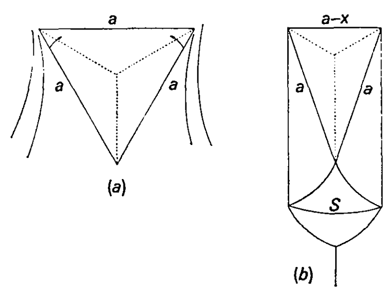

Fig. 5. Diagrams showing schematically the conversion of an equilateral trigon (*a*) into an isosceles triangle (*b*) with the base shorter than the other sides.

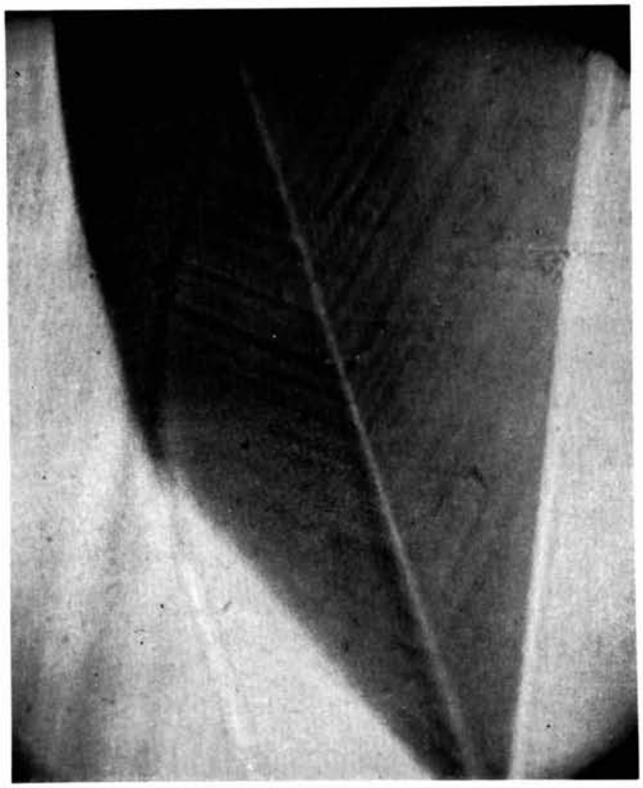

Fig. 1. The wing of a trigon (× 1000).

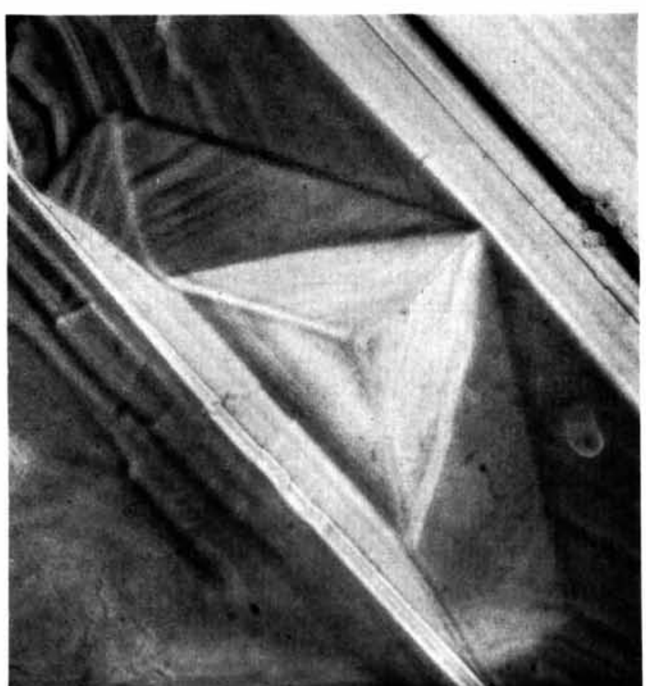

Fig. 2. Isosceles trigon with base longer than the other sides (× 395).

]To face p. 708

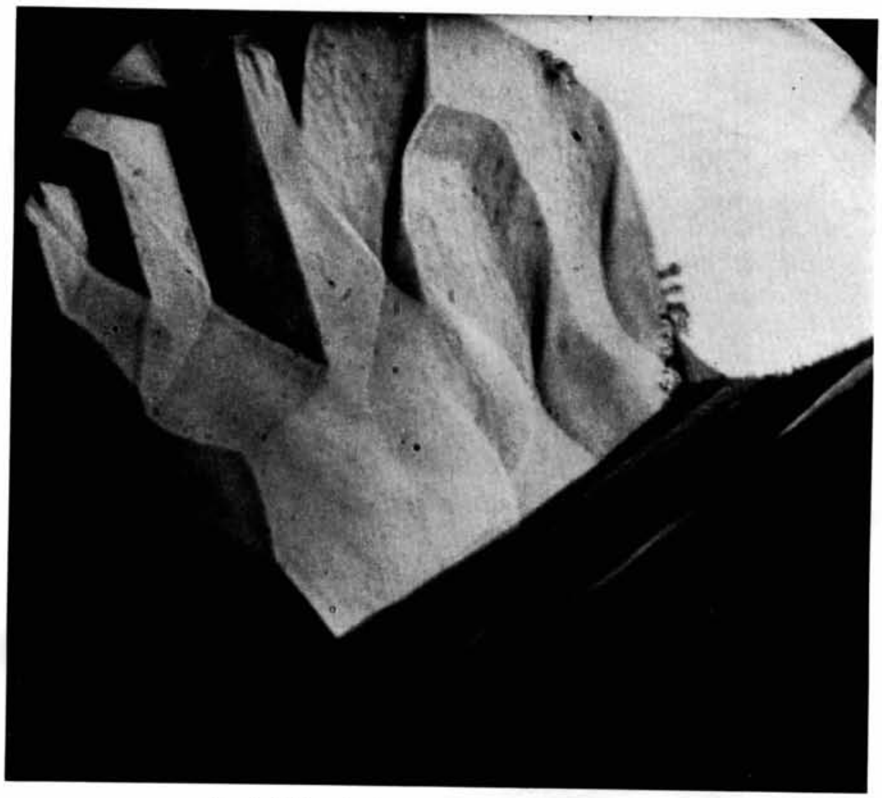

Fig. 4. Winged trigon and fish shape (× 350).

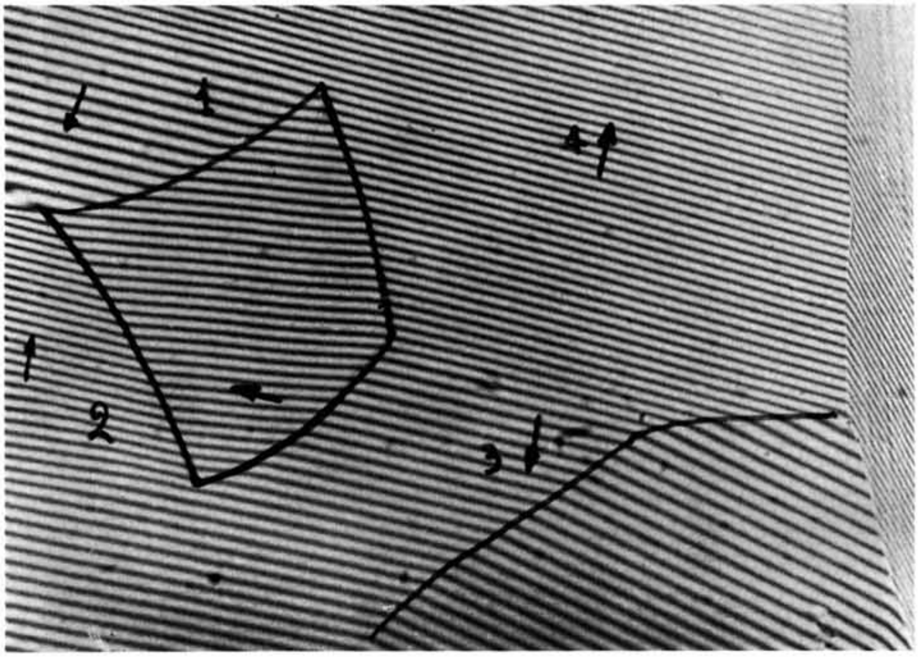

Fig. 6. Interferogram of features of the (111) face ($\times$ 700).

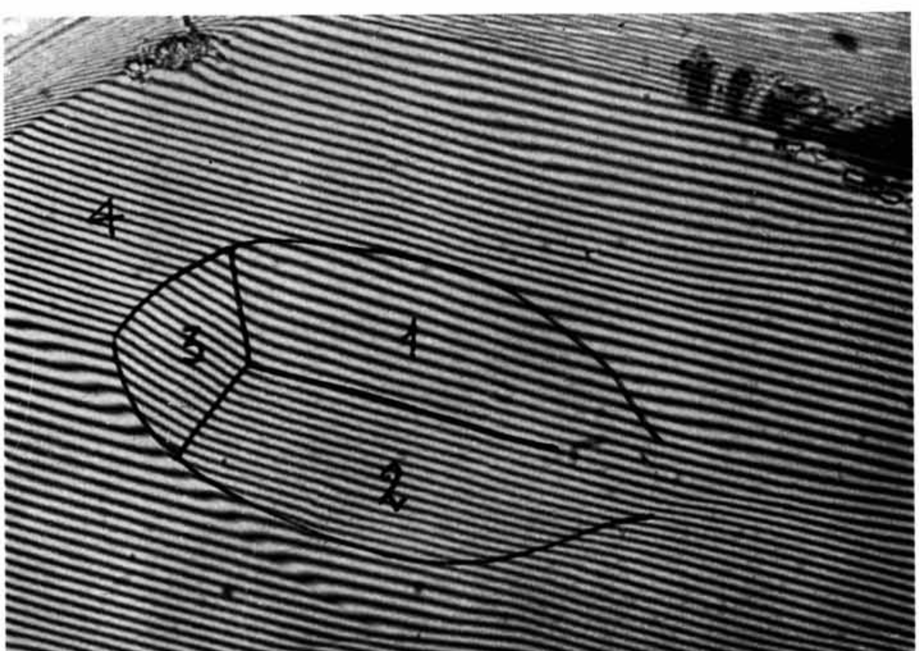

Fig. 7. Interferogram of the fish shape ($\times$ 700).

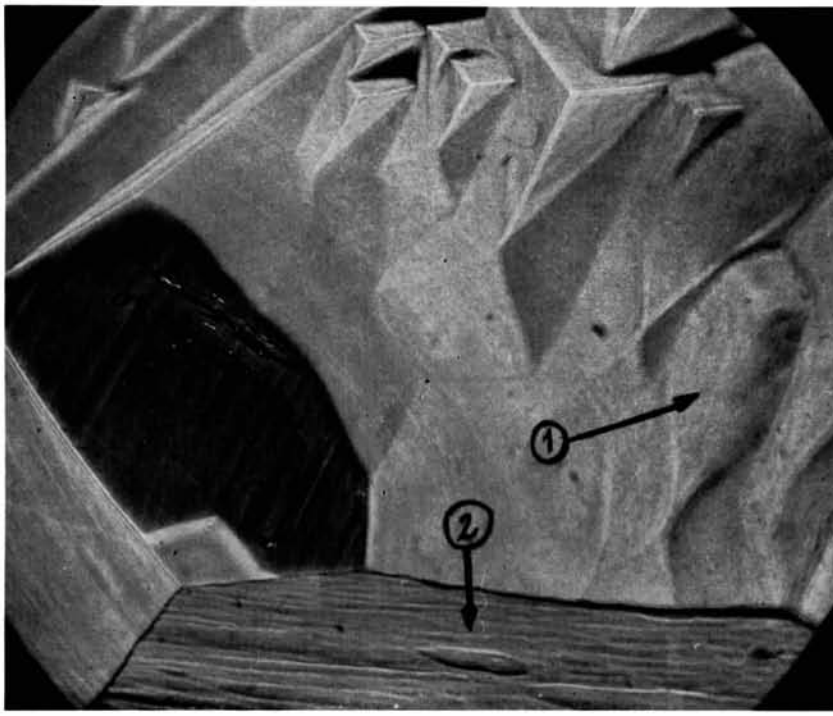

Fig. 8. Fish shape (1) and boat shape (2) × (315).

Fig. 10. Growth layers on the (111) face (× 395).

their ends to build up half of the vicinal face (S in the illustration).

This vicinal face S has a quadrangular shape, is not quite plane, and is an (hhl) vicinal face of the icositetrahedral type.

The interferogram of Fig. 6 shows clearly the slope of this vicinal face. The zones of interest have been outlined in ink to make the pattern clearer. There are four zones. Each zone has a uniform slope as shown by the packing of the fringes: 1 and 2 correspond to the wings of the trigon. The quadrangular shape and the surfaces 3 and 4 build up a very flat pyramid with vicinal faces of the icositetrahedron type. The arrows indicate approximately the slopes of the surfaces, and this is confirmed by the clear and dark corresponding zones of Fig. 4 in the upper left part (phase contrast).

A further interesting zone is shown by the fish-like shape in the upper right part of Fig. 4. An interferogram over this shape outlined in ink shows that is a depression (Fig. 7); it is possible to note by the packing of the fringes that the slopes of the sides 1 and 2 are the same (or very nearly the same) as those in zones 1 and 2 of Fig. 6, the wings of the trigon.

An experimental check has been made on many wing trigons. They may also be formed when not in the presence of two contiguous trigons as some authors have suggested (Berman, 1965). Wings can also appear on isolated trigons, and layers of the same type and with the same orientation appear without any trigon at all.

Discussion

From many photographs, it is possible to derive certain conclusions as follows.

It is reasonable to infer that a strict correlation does exist between the formation of the layers and the changing of shape of the trigon. As a result of the fresh arrival of new material a trigon tends to disappear through the building up of vicinal faces of a slope smaller than that of the sides of the trigon. The sides of the trigon may still be considered as vicinal faces.

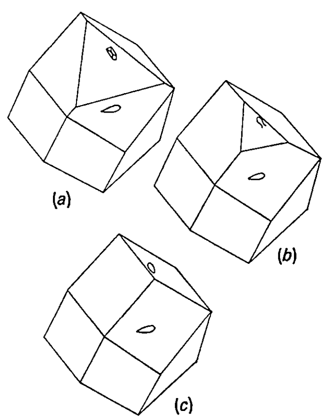

Fig. 9. Schematic illustration of (*a*) isosceles trigon, (*b*) fish shape and (*c*) boat shape as successive stages in growth.

With respect to the isosceles trigon and the 'fish' shape on its right (Fig. 4), from the interferograms of Figs. 6 and 7 it is seen that the slopes of the sides 1 and 2 of the 'fish' shape are the same as the corresponding slopes 1 and 2 of the wings of the isosceles trigon. It is reasonable to think that in Fig. 7 the two wings of a pre-existing trigon have filled up a trigon completely while the third face of the trigon has grown meanwhile to build up a vicinal face of the (hhl) type. In the 'fish' shape of Fig. 4, the pyramidal edges (directed downwards) of the pre-existing trigon are still visible. All this suggests that the isosceles trigon and the 'fish' shape are successive stages of the same process. As supporting evidence it can be noted that the partially filled up trigons, on the sides of which the wings are attached, sometimes have different slopes, the smaller slope being that near the wing.

It may be argued too, that the isosceles trigon with a larger base (Fig. 2) is in the initial stage of a filling-up process, which will proceed with a symmetry different from the previous one.

If the isosceles trigon with small base is considered as a first stage of the growth, the 'fish' shape may be the second stage in the further filling up due to the fresh arrival of growth material. It is possible that the 'fish' shape may become the 'boat' shape so often seen on a rhombic dodecahedral face. This is also suggested by the relative orientation between 'fish' shape and 'boat' shape as seen in Fig. 8. This sequence is schematically drawn in Fig. 9.

This evolution is comparable to the evolution of the last stage of the growth suggested in the previous paper (Bedarida & Komatsu, 1965), the presence of $\{hhl\}$ forms generated differently from those described there now confirming the transformation $\{111\} \rightarrow \{hhl\} \rightarrow \{110\}$.

The above view does not agree with the opinion of Orlov (1963), who states that the boat shapes are hillocks derived by partial dissolution from pyramids. The present observations on the contrary reveal that the boat shapes are always depressions.

If the rhombic dodecahedron faces are etched, boat shapes again appear (Tolansky, 1955) and it may be thought that the two mechanisms, growth and etching, are directly correlated.

It may be pointed out again that these shapes have only been seen on the periphery of the crystal, agreeing with what Orlov states on this point.

The observations described here and in the previous publication support the hypothesis that the patterns reported are due to growth. It appears very difficult to explain these various phenomena in terms of etching: in the process shown schematically in Figs. 3 and 5 it does not seem possible to arrive at any explanation by reversing the evolution to be that of a solution process.

The case in which, on the addition of the layers, the trigon edges have remained equilateral, supports the suggestion made some years ago by Tolansky &

Wilcock (1946) that the layers have stopped on arriving at the side of a trigon. Very probably this is true only when the layers are thicker than a certain value.

The writer wishes to thank Professor S. Tolansky for hospitality in his laboratory, where part of this work was done, and for many useful suggestions, Professor E. Sanero for his constant support and interest in the work, and Doctor H. Komatsu for some discussions on the subject.

References

BEDARIDA, F. & KOMATSU, H. (1966). *Acta Cryst.* **21**, 276.
BERMAN, R. (1965). *Physical Properties of Diamond.* p. 90–91. Oxford: Clarendon Press.
ORLOV, YU. L. (1963). *Morphology of Diamonds.* p. 153, Fig. 126. Moscow: U.S.S.R. Academy of Science.
TOLANSKY, S. (1955). *Microstructures of Diamond Surfaces.* Plate 86. London: N.A.G. Ltd.
TOLANSKY, S. & WILCOCK, W. L. (1946). *Nature, Lond.* **157**, 583.

Acta Cryst. (1967). **23**, 710

The Equation of Kikuchi Lines on the Basis of the Kikuchi Geometrical Model

BY MICHAL LENC

Institute of Instrument Technology, Laboratory of Electron Optics, Czechoslovak Academy of Sciences, Brno, Czechoslovakia

(*Received* 30 *December* 1966)

The applicability of the Kikuchi model of the origin of P patterns in electron diffraction is discussed. With the use of this model the equation of Kikuchi lines is derived and examples are given of crystallographic measurements carried out with high accuracy by means of this equation.

Introduction

Various electron diffraction patterns for the case of a single crystal have been investigated. These can be conventionally classified into three types: N, L and P (Pinsker, 1949).

Kikuchi (1928) proposed a geometrical model (Fig. 1) which is very simple but seems to be useful for describing the geometry of P patterns. Finch, Quarell & Wilman (1935), Finch & Wilman (1936), and Wilman (1948) described some possibilities of this model. In the present paper we give (1) the derivation of the equation of Kikuchi lines for an arbitrary experimental arrangement and (2) some examples of the practical applications of this equation.

Applicability of the Kikuchi model

Using the Kikuchi model we suppose the primary wave to be scattered by the first (upper) part of a thick crystal. The wave packet is obtained the wave vectors of which lie in a small solid angle in the vicinity of the direction of the incident wave. This wave packet is diffracted by the second (lower) part of the crystal. The well-known condition for the maximum of the intensity with respect to the crystal position (resulting from the diffraction theory at Born approximation) (Bohm, 1958)

$$\mathbf{K}_0 - \mathbf{K} = \mathbf{H} \tag{1}$$

reduces then to

$$|\mathbf{K}_0||\mathbf{K}| \cos (\mathbf{K}_0,\mathbf{K}) - \mathbf{K}^2 = \mathbf{HK}\,. \tag{2}$$

Here $\mathbf{K}_0$, $\mathbf{K}$, $\mathbf{H}$ are vectors of the incident and diffracted waves and of the reciprocal lattice, respectively.

It is a matter of dynamical theory to give the limits for the validity of this model. But it seems clear we can use the model for the case of a thin crystal. Here the experiment may be arranged in such a way that we produce a suitable wave packet by means of an electron lens and we allow this packet to be diffracted by a crystal (Kossel & Möllenstedt, 1942).

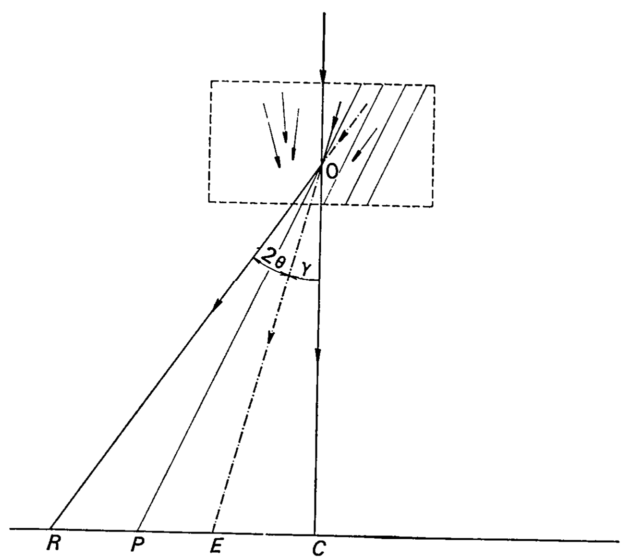

Fig. 1. Kikuchi geometrical model.